information

MDPI

Article

Automatic Hemiplegia Type Detection (Right or Left) Using the Levenberg-Marquardt Backpropagation Method

Vasileios Christou [1,*], Alexandros Arjmand [1], Dimitrios Dimopoulos [2], Dimitrios Varvarousis [2], Ioannis Tsoulos [1], Alexandros T. Tzallas [1], Christos Gogos [1], Markos G. Tsipouras [3], Evripidis Glavas [1], Avraam Ploumis [2] and Nikolaos Giannakeas [1,*]

1 Department of Informatics and Telecommunications, University of Ioannina, GR47100 Arta, Greece; alexarjmnd@gmail.com (A.A.); itsoulos@gmail.com (I.T.); tzallas@uoi.gr (A.T.T.); cgogos@uoi.gr (C.G.); eglavas@uoi.gr (E.G.)
2 Department of Physical Medicine and Rehabilitation, University of Ioannina, S. Niarchos Ave, GR45110 Ioannina, Greece; ddimop@uoi.gr (D.D.); dimvarvar@gmail.com (D.V.); aploumis@uoi.gr (A.P.)
3 Department of Electrical and Computer Engineering, University of Western Macedonia, GR50100 Kozani, Greece; mtsipouras@uowm.gr
* Correspondence: bchristou1@gmail.com (V.C.); giannakeas@uoi.gr (N.G.)

Abstract: Hemiplegia affects a significant portion of the human population. It is a condition that causes motor impairment and severely reduces the patient's quality of life. This paper presents an automatic system for identifying the hemiplegia type (right or left part of the body is affected). The proposed system utilizes the data taken from patients and healthy subjects using the accelerometer sensor from the RehaGait mobile gait analysis system. The collected data undergo a pre-processing procedure followed by a feature extraction stage. The extracted features are then sent to a neural network trained by the Levenberg-Marquardt backpropagation (LM-BP) algorithm. The experimental part of this research involved creating a custom-created dataset containing entries taken from ten healthy and twenty non-healthy subjects. The data were taken from seven different sensors placed in specific areas of the subjects' bodies. These sensors can capture a three-dimensional (3D) signal using the accelerometer, magnetometer, and gyroscope device types. The proposed system used the signals taken from the accelerometers, which were split into 2-sec windows. The proposed system achieved a classification accuracy of 95.12% and was compared with fourteen commonly used machine learning approaches.

Keywords: accelerometer; feature extraction; hemiplegia; Levenberg-Marquardt backpropagation; neural network

Citation: Christou, V.; Arjmand, A.; Dimopoulos, D.; Varvarousis, D.; Tsoulos, I.; Tzallas, A.T.; Gogos, C.; Tsipouras, M.G.; Glavas, E.; Ploumis, A.; et al. Automatic Hemiplegia Type Detection (Right or Left) Using the Levenberg-Marquardt Backpropagation Method. *Information* **2022**, *13*, 101. https://doi.org/10.3390/info13020101

Academic Editor: Arkaitz Zubiaga

Received: 20 December 2021
Accepted: 17 February 2022
Published: 21 February 2022

1. Introduction

Hemiplegia is a disease that causes the patient to lose motor control in one part of the body. The hemiplegia symptoms include the patient's inability to move its right or left body parts (arm and leg) and the creation of spastic mass patterns. The paralysis in half of the patient's body is usually caused by a stroke and has severe consequences on their health and quality of life. It is an effect caused by damage in one of the two cerebral hemispheres. The problems caused by a brain lesion in one area are spread to other areas since the human brain is an extensive network of interconnected neurons participating in two different types of communication (feed-forward and feedback). The unaffected areas of the brain face problems due to the lack of information or misinformation created from the affected areas. The stroke patient will have to deal with severe problems in both body sides, with side effects spreading to all brain functions causing motor impairment in the whole body. These impairments will affect sensory perception, memory, and behavior, causing a challenging situation to the patient's rehabilitation process. Hemiplegia types can be right or left, as seen in Figure 1. In the former type, the left body side is paralyzed,

while in the latter type, the right body side is paralyzed. An example causing either type is an incomplete spinal cord injury [1,2].

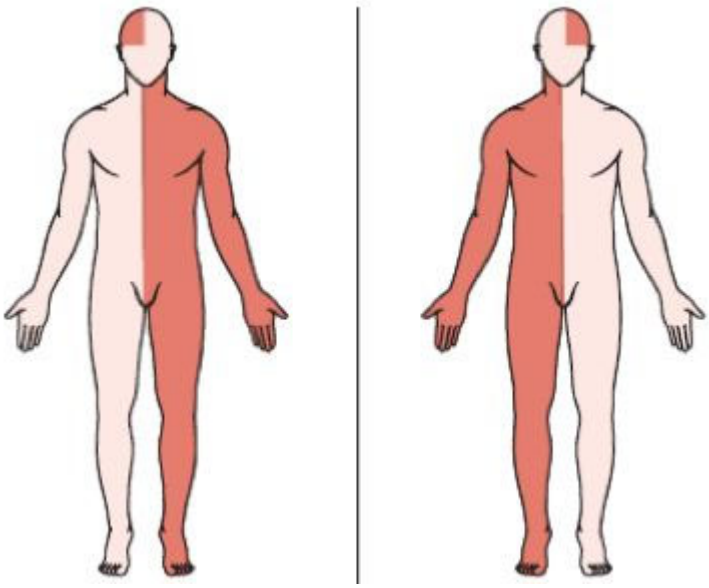

Figure 1. Hemiplegia types. The left picture depicts brain damage in the left part of the brain (all the affected body parts are marked with red color), which causes paralysis to the right part of the body. The right picture depicts brain damage in the right part of the brain, which causes paralysis to the right part of the body.

The novelty behind the proposed system is creating a tool capable of detecting the hemiplegia category (right or left) between patients and healthy individuals using a low-cost system that doesn't require the use of an expensive three-dimensional (3D) camera. The proposed method can be used as a supplementary tool for diagnosing the hemiplegia types mentioned above amongst patients and healthy subjects. The system works by using seven sensors to the subject's body which record Spatio-temporal specific parameters during walking. One sensor is placed on the hip, and one is placed at each patient's foot, shank, and thigh. All the sensors are provided from the RehaGait mobile gait analysis system [3–5].

The mobile gait analysis system offers significant advantages, including monitoring the user's status using a built-in video capture feature. It can recognize the damaged areas, estimate the gait pattern and find asymmetries in the patient's lower limbs. The rest of its advantages include movement freedom, mobility since it does not require a gait lab, and the ability to represent the captured data graphically [5,6].

The sensors can capture 3-dimensional (3D) signals using an accelerometer that records the linear acceleration, a magnetometer that records the earth's magnetic, and a gyroscope for recording the angular velocity [4]. The proposed method used the captured accelerometer data, divided into widows with a 2-s length. Then, they underwent a pre-processing and feature extraction stage before being sent to a single-layer neural network trained by the Levenberg-Marquardt backpropagation (LM-BP) algorithm. The training procedure of the neural network involved using a custom dataset that contained data taken from thirty participants (twenty non-healthy individuals having right or left hemiplegia and ten healthy individuals).

The article is structured in seven sections. It begins with the "Introduction" section, which includes the problem's description and the motivation, followed by the "Related Work" section. "The LM-BP Algorithm" section describes the architecture of the Levenberg-Marquardt backpropagation variant utilized for the classification task of the proposed method. The "System Architecture" section describes an analysis of the system. The "Experimental Results" section contains the outcome from comparing the proposed ap-

proach with fourteen machine learning algorithms. Finally, the last two sections contain the "Discussion" and "Conclusion."

2. Related Work

The existing bibliography includes methods targeted to different hemiplegia aspects, including gait. Lee et al. [6] created a classification method based on the random forests (RFs) algorithm for distinguishing between hemiplegic and non-hemiplegic gait. The system utilizes the acceleration signal captured from a wearable device. Ji et al. [7] studied the efficiency of various mother wavelets and wavelet selection criteria in gait event detection using hemiplegic and non-hemiplegic patients. Pauk and Minta-Bielecka [8] proposed a biclustering algorithm for classifying gait patterns in hemiplegia patients. Their method is based on the study of clustering and biclustering approaches. Patil et al. [9] used deep learning and CNNs for the analysis of human gait with the purpose of identifying hemiplegic gait Padilla [10] created a fuzzy modeling of the hemiplegic indicators in patients' knees to classify hemiplegic gait. Manca et al. [11] utilized a hierarchical cluster analysis method to classify the gait patterns from 49 hemiplegic individuals having equinous foot deformity. Kim et al. [12] utilized the Vicon® 512 motion analysis system to compare the gait of hemiplegic elderly individuals and healthy subjects of similar age. LeMoyne et al. [13] utilized logistic regression for distinguishing between an affected and unaffected hemiplegic leg pair using the features taken from force plate data. The analysis revealed five groups with homogenous gait dysfunction levels. Jung et al. [14] created a gait rehabilitation system controlled by a deep neural network (DNN) to offer functional electric stimulation to individuals suffering from hemiplegia. This study showed that the performance of the proposed gait event detection method based on continuous wavelet transform was affected by the use of different mother wavelet functions. Yardimci [15] utilized fuzzy logic with the Tsukamato-type inference method to classify hemiplegic and healthy individuals. Luo and Luo [16] used kinematic data from 8 hemiplegic patients to estimate the intra-limb coordination of the lower limb. Wong et al. [17] explored the possibility of using a foot contact pattern for neurologic recovery prediction and how ambulation training affects individuals suffering from hemiplegia. LeMoyne and Mastroianni [18] utilized a multi-layer perceptron neural network to classify an affected and unaffected leg in hemiplegic gait. The system uses a smartphone as a wearable device and utilizes its gyroscope sensor signal data which undergo a feature extraction stage before being sent as input to the neural network.

Many studies utilized data taken from hemiplegic children. Aguilera and Subero [19] studied kinematic, kinetic, and electromyographic (EMG) data from children having spastic hemiplegia. The purpose of their work was to find meaningful patterns in gait. Morbidoni et al. [20] proposed a machine learning method for binary classification of gait and heel-strike (HS), and toe-off (TO) timing prediction from surface electromyographic (sEMG) signals in cerebral palsy hemiplegic children. Agostini and Nascimberi [21] explored muscle activity and various foot-floor contact patterns during gait in hemiplegia children. Utilizing statistical gait analysis, they received the foot-floor contact patterns end estimated the gait phases duration. They also used a user-independent method for receiving the muscle activation timing for every foot-floor contact sequence and muscle activation pattern. Di Nardo et al. [22] quantified the asymmetric behavior of 16 children with mild hemiplegia during walking by using surface-EMG and foot-floor contact features. McAloon et al. [23] validated the activPAL activity monitor in children with hemiplegic gait. Krzak et al. [24] studied the effect in gait patterns of fine wire insertion into the posterior tibialis muscle in children with hemiplegic cerebral palsy. Wang and Wang [25] performed a gait analysis in healthy children and children having spastic hemiplegic cerebral palsy. Aguilera et al. [26] studied various data mining methods in gait data taken from children having spastic hemiplegia. Abaid et al. [27] proposed a hidden Markov model-based gait phase detection algorithm using data taken from single-axis wearable gyroscopes. The algorithm can differentiate between typically developing and hemiplegic children and estimates the gait ability level in non-healthy subjects.

Some studies were focused on creating an evaluation system. Watanabe and Miyazawa [28] developed a stride length measurement-based gait evaluation system that utilizes inertial sensors. The proposed system was tested with healthy and hemiplegic patients with and without functional electrical stimulation-assisted foot drop correction. Granat et al. [29] proposed a hemiplegic gait evaluation system that utilizes shoe insoles equipped with sensors. The system can monitor the patient's gait for 10 min and is usable on any surface. Ohnishi et al. [30] created an automatic evaluation system for stroke impairment analysis set (SIAS) utilizing depth sensors. SIAS is a collection of evaluation methods for hemiplegic patients who suffered a stroke.

Many studies proposed classification systems aimed to recognize two or more neurodegenerative diseases. Kumari et al. [31] created a wearable human activity tracking device used in patients with spastic hemiplegia and diplegia. Li et al. [32] utilized a 3D human skeleton and a Kinect sensor to capture the joints' trajectories with the purpose of recognizing Parkinson's disease and hemiplegia. Pandit et al. [33] captured the data from four body adhering modules and converted them into images which were introduced to an Inception v3 convolutional neural network (CNN). The network was responsible for classifying those images into four gait categories (normal, hemiplegic, diplegic, and Parkinsonian).

Other hemiplegia-based approaches include the hand gesture recognition system by Azlan et al. [34] for rehabilitating people suffering from hemiplegia by stimulating motor function. Cai et al. [35] utilized a pressure distribution mattress to create a compensatory movement pattern detection system in stroke patients with hemiplegia. For the participants' classification task of the posture, the following four machine methods were utilized: linear discriminant analysis (LDA), k-nearest neighbors, naïve Bayes, and support vector machine (SVM).

The methods described above showed very good results, but they were not focused on the hemiplegia type detection (right or left), which motivated the proposed work. One exception is the work from Christou et al. [36], which utilizes a neural network trained with the scaled conjugate gradient backpropagation (SCG-BP) training algorithm. The neural network can detect the hemiplegia category (right or left) between patients and healthy subjects. Although this method manages to get a high classification accuracy, the LM-BP-based method proposed in this article gets a higher classification accuracy than the SCG-BP approach.

Other works include the feature extraction method by Priya et al. [37], which aims to recognize Parkinsonian gait. The proposed symmetrically weighted local neighbor gradient pattern (SWLNGP) method analyzes signals taken from human gait using local binary pattern (LBP) techniques during the feature extraction stage. Then, it classifies them with the help of an artificial neural network (ANN).

The data classification task is a critical part of the LM-BP-based system presented in this article. A few typical BP-based machine learning methods for this task are described below. The SCG-BP training algorithm by Møller [38] is a variation of the original backpropagation (BP) algorithm which utilizes a Levenberg-Marquardt approach for the elimination of the computationally-intensive line search [39,40]. Fletcher-Powell conjugate gradient BP (FPCG-BP) is a conjugate gradient-based approach that utilizes the Fletcher-Reeves updates to update the weights and thresholds [41]. The Broyden, Fletcher, Goldfarb, and Shanno backpropagation (BFGS-BP) method is a quasi-Newton approach for unconstrained optimization problems which utilizes updating formulas for the Hessian approximation [42]. The one-step secant backpropagation (OSS-BP) algorithm fills the gap between the conjugate gradient approaches and the quasi-Newton algorithms. One-step secant assumes that the previous Hessian is the identity matrix at each epoch. This assumption has the advantage that the new search direction can be calculated without the help of the matrix inverse, which makes it require less storage space and is faster than the BFGS method [43]. Gradient descent (GD) is an iterative optimization algorithm that utilizes first-order derivatives to find a local minimum of a differentiable function [44]. A major issue with gradient descent, when used to train a multi-layer network with a sigmoid transfer function, is that the gradient has a very small magnitude that causes small changes in the weights and

thresholds, which slows down the training process. Resilient propagation (RPROP) was developed to solve the above problem and works by using a local adaptation of the weight updates following the error function's behavior [45]. The Bayesian regularization back-propagation (BR-BP) algorithm modifies and minimizes a linear combination of squared errors and weights. The purpose of the resulting network is to achieve good generalization performance [46,47]. Root mean squared propagation (RMSProp) [48] extends gradient descent and the AdaGrad version of gradient descent. It utilizes a decaying average of partial gradients to adapt the step size in each parameter. The Adam optimizer [49] is a first-order gradient-based optimization method for stochastic objective functions which utilizes adaptive estimates of lower-order moments. The AdaMax [49] algorithm is an extension of Adam based on the infinity norm. The adaptive gradient (AdaGrad) algorithm [50] scales the learning rate parameter for each dimension in an adaptive manner to certify that the training process is not too slow and not too volatile and imprecise.

Other non-BP approaches include the extreme learning machine (ELM) proposed by Huang et al. [51], which can train a single-layer neural network (SLNN) without the use of an iterative training method like traditional learning algorithms. ELM training process involves randomizing the hidden layer weight and thresholds followed by an analytical determination of the output weights. Optimally pruned ELM (OP-ELM) proposed by Miche et al. [52] is an ELM-based approach that creates a large SLNN and evaluates each hidden layer node using the multi-response sparse regression algorithm. Then, it selects the best neurons, which will form the final network. Finally, the SVM algorithm creates optimal separating hyperplanes in a high or infinite-dimensional space utilized for classification or regression tasks of unknown data [53].

3. The LM-BP Algorithm

This section represents a detailed explanation of the LM algorithm. The LM algorithm was initially developed by Kenneth Levenberg [39] and reinvented by Donald Marquardt [40] to minimize a non-linear function.

The LM Algorithm has $O\left(N^3\right)$ complexity and is illustrated in Algorithm 1 [54]. The algorithm trains a neural network by adapting the network's weights and thresholds according to the weight update function depicted in (1).

$$w_{k+1} = w_k - \left(J_k^T J_k + \mu I\right)^{-1} J_k e_k \tag{1}$$

The first five lines of the algorithm initialize its parameters. These initializations include:

- Randomizing weights and thresholds.
- Setting the maximum number of steps, the initial value of the learning coefficient, and the maximum allowed sum of squares network error.

Line 6 declares the neural network inputs. Line 7 starts the algorithm's epochs, and line 8 resets the current step number iterator for each epoch. The next step calculates the neural network output, while the formula in line 10 defines the sum of squares error for the whole network. The next line involves calculating the Jacobian matrix J, used in the weight and threshold update function (line 12). Line 13 calculates the neural network output using the updated weights and thresholds. The next step calculates the updated sum of squares error for the whole network, used as a stopping criterion for the algorithm. If the error is larger than the previous error, the LM method checks if $m \leq m_{max}$ (lines 15, 16). If the latter condition is satisfied, then m is increased by one, and the learning coefficient is multiplied by a factor of 10 (lines 17, 18). Then, the previous weight and threshold updates are retracted, and a new update is calculated considering the new learning coefficient (line 19). On the other hand, if the maximum allowed number of steps has been exceeded ($m > m_{max}$) the weight and threshold update procedure is accepted, and a new training epoch begins (line 21). If the error is smaller than the previous error, μ is reduced by a factor of 10, the weight and threshold update procedure is accepted, and a new training

epoch begins (lines 24, 25). Finally, the training epochs continue until the stopping criterion is satisfied (line 27) and the neural network output (y) is returned (line 28).

Algorithm 1: The Levenberg-Marquardt Algorithm

1: $w_1 \dots w_N \in \mathbb{R},\ N \in \mathbb{N}^*$
2: $b_1 \dots b_N \in \mathbb{R},\ N \in \mathbb{N}^*$
3: $m_{max} \in \mathbb{N}^*$
4: $\mu \in \mathbb{R}^*$
5: $E_{max} \in \mathbb{R}^*$
6: $x = \begin{bmatrix} x_{11} & \cdots & x_{1n} \\ \vdots & \ddots & \vdots \\ x_{N1} & \cdots & x_{Nn} \end{bmatrix}_{N \times n} \in \mathbb{R},\ n \in \mathbb{N}^*, N \in \mathbb{N}^*$
7: do
8: $m = 1$
9: $y = net(wb_k, x)$
10: $E_k = \sum_{i=1}^{n} (t_i - y_i)^2$
11: $J = \begin{bmatrix} \frac{\partial e_{1,1}}{\partial w_1} & \frac{\partial e_{1,1}}{\partial w_2} & \cdots & \frac{\partial e_{1,1}}{\partial w_N} & \frac{\partial e_{1,1}}{\partial b_N} \\ \frac{\partial e_{1,2}}{\partial w_1} & \frac{\partial e_{1,2}}{\partial w_2} & \cdots & \frac{\partial e_{1,2}}{\partial w_N} & \frac{\partial e_{1,2}}{\partial b_N} \\ \cdots & \cdots & \cdots & \cdots & \cdots \\ \frac{\partial e_{1,M}}{\partial w_1} & \frac{\partial e_{1,M}}{\partial w_2} & \cdots & \frac{\partial e_{1,M}}{\partial w_N} & \frac{\partial e_{1,M}}{\partial b_N} \\ \cdots & \cdots & \cdots & \cdots & \cdots \\ \frac{\partial e_{P,1}}{\partial w_1} & \frac{\partial e_{P,1}}{\partial w_2} & \cdots & \frac{\partial e_{P,1}}{\partial w_N} & \frac{\partial e_{P,1}}{\partial b_N} \\ \frac{\partial e_{P,2}}{\partial w_1} & \frac{\partial e_{P,2}}{\partial w_2} & \cdots & \frac{\partial e_{P,2}}{\partial w_N} & \frac{\partial e_{P,2}}{\partial b_N} \\ \cdots & \cdots & \cdots & \cdots & \cdots \\ \frac{\partial e_{P,M}}{\partial w_1} & \frac{\partial e_{P,M}}{\partial w_2} & \cdots & \frac{\partial e_{P,M}}{\partial w_N} & \frac{\partial e_{P,M}}{\partial b_N} \end{bmatrix} P \in \mathbb{N}^*,\ M \in \mathbb{N}^*$
12: $wb_{k+1} = wb_k - \left(J_k^T J_k + \mu I\right)^{-1} J_k e_k$
13: $y = net(wb_{k+1}, x)$
14: $E_{k+1} = \sum_{i=1}^{n} (t_i - y_i)^2$
15: if $E_{k+1} > E_k$
16: if $m \leq m_{max}$
17: $m = m + 1$
18: $\mu = 10\mu$
19: $wb_{k+1} = wb_k - \left(J_k^T J_k + \mu I\right)^{-1} J_k e_k$
20: else
21: $wb_k = wb_{k+1}$
22: end if
23: else
24: $\mu = \frac{\mu}{10}$
25: $wb_k = wb_{k+1}$
26: end if
27: while $E_{k+1} > E_{max}$
28: return y

4. System Architecture

The architectural structure of the system utilizes the RehaGait mobile gait analysis system [3,4], containing seven sensors that can be placed at various patient body parts. Every sensor contains an accelerometer, a magnetometer, and a gyroscope. The proposed system utilizes the accelerometer signals, which are windowed into 2-s windows and undergo a pre-processing and feature extraction stage. The signals are transmitted wirelessly from the RehaGait mobile gait analysis system to a laptop, responsible for the pre-processing, feature extraction, and classification tasks. The pre-processing stage involves using a low-pass filter to smooth the signal.

The feature extraction stage involves using four time-domain features and two frequency-domain features. The first from the time-domain features is the mean (μ) seen below where N denotes the number of scalar observations and A is a random variable vector.

$$\mu = \frac{1}{N}\sum_{i=1}^{N} A_i \tag{2}$$

The second feature was the standard deviation shown in Formula (3), where N is the number of scalar observations, A is a random variable vector, and μ is the mean of A.

$$S = \sqrt{\frac{1}{N-1}\sum_{i=1}^{N}(A_i - \mu)^2} \tag{3}$$

The third feature is the kurtosis of a distribution depicted in Equation (4) where $E(t)$ denotes the expected value of quantity t, μ is the mean of x and σ is the standard deviation of x.

$$k = \frac{E(x-\mu)^4}{\sigma^4} \tag{4}$$

The fourth feature is the peak-magnitude-to-RMS ratio depicted in Equation (5).

$$\text{RMS} = \frac{\|A\|_\infty}{\sqrt{\frac{1}{N}\sum_{i=1}^{N}|A_i|^2}} \tag{5}$$

Regarding the frequency-domain features, the acceleration energy and the acceleration signal energy are selected. The first one is described in Equation (6) with A_i defining the i^{th} spectral line of the acceleration signal and N the total lines.

$$Eng = \frac{\sum_{i=1}^{N} A_i^2}{N} \tag{6}$$

The last feature is the acceleration signal entropy seen below with p_i defining the probability of the A_i value occurring in the amplitude spectrum.

$$Ent = -\sum_{i=1}^{N} p_i \log_2 p_i \tag{7}$$

The above six features formed the feature vector sent as input to a neural network trained with the LM-BP algorithm. The motivation behind selecting those features was the reduction of the initial large dataset to a smaller dataset that can be easily transferred and processed with a low-cost credit card type computer like Raspberry Pi Zero W. Moreover, the above feature combination achieved the highest classification accuracy over alternative ones containing different feature sets. The neural network classified the input data into three classes (healthy, left, or right hemiplegia). The data were taken from a custom-created dataset divided into training, validation, and a separate test set. The k-fold cross-validation method was utilized in the training and validation sets. A visualization of the proposed system can be seen in Figure 2.

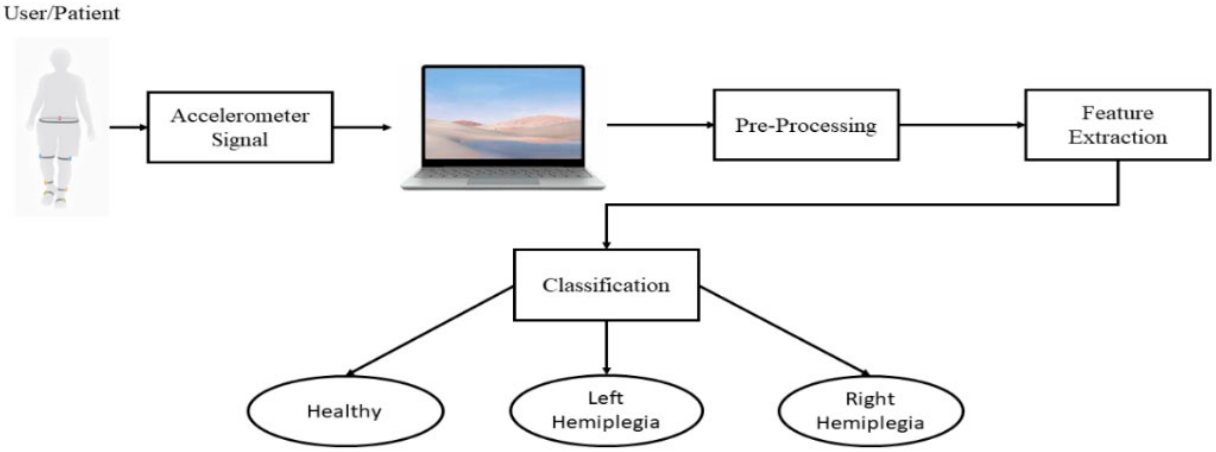

Figure 2. The system architecture. The system receives the accelerometer signals from seven sensors placed in various body parts, which undergo a pre-processing and feature extraction procedure. Then, the extracted features are sent as input to a neural network trained with the LM-BP algorithm responsible for their classification into three classes (healthy, left, or right hemiplegia).

5. Experimental Results

The proposed LM-BP-based system was tested using data from ten healthy, eight non-healthy subjects having left hemiplegia and twelve non-healthy subjects having right hemiplegia. The study was conducted according to the guidelines of the Declaration of Helsinki and approved by the Ethics Committee of the University of Ioannina. Informed consent was obtained from all subjects involved in the study, and written informed consent was obtained from the patients to publish this paper. The signals from the seven accelerometers were sent wirelessly to a laptop and were divided into 2-s windows. The windowed signals underwent a pre-processing phase using a low pass filter and a feature extraction process according to the procedure described in the previous section. These features were sent to a neural network trained with the LM-BP algorithm. The architecture of the neural network involved the creation of one hidden layer with 30 neurons having the sigmoid $\left(y = \frac{1}{1+e^{-x}}\right)$ transfer function and three output layer neurons with the identity $(y = x)$ transfer function with each input vector containing 126 values (6 features $\times$ 7 accelerometers $\times$ 3 dimensions).

The proposed system was tested with the following fourteen machine learning approaches:

- SCG-BP
- FPCG-BP
- BFGS-BP
- OSS-BP
- GD-BP
- RPROP
- BR-BP
- RMSProp
- Adam
- AdaMax
- AMSGrad
- ELM
- OP-ELM
- SVM

The motivation behind comparing the LM-BP algorithm with other BP variants was to evaluate its accuracy compared to other alternative BP-based solutions. The accuracy level achieved by LM-BP was also higher compared to other non-BP-based solutions like SVM,

ELM, and OP-ELM. ELM and OP-ELM are relatively new SLNN training methods that can train SLNNs faster than other iterative-based methods.

The experiments were run ten times for all neural network-based approaches to avoid any bias due to the random initialization of the hidden weights and thresholds. In the RMSProp, Adam, AdaMax, AMSGrad, ELM-based, and SVM methods, 20% of the dataset was kept as a test set, and the rest was used as a training set. In the other approaches, 20% of the dataset was kept as a test set, and the rest was further divided into training and validation sets using 10-fold cross-validation. The RMSProp, Adam, AdaMax, and AMSGrad approaches were run for 500 epochs. The dataset contained 2036 entries, with 1630 rows forming the training/validation sets and 406 entries the test set. All neural networks had one hidden layer with thirty nodes. The parameters for all the experiments are summarized below. The heterogenous OP-ELM algorithm was used with three different types of kernels (linear, Gaussian, and sigmoid). The parameters for the execution of the experiments can be seen in Table 1.

Table 1. Parameter Values.

Parameter Name	Value
Experiment Repeats	10
Hidden Layer Nodes No	30
Output Layer Nodes No	3
Input Vector Size	126
Test Set Size	20%
RMSProp, Adam, AdaMax and AMSGrad Epochs No	500
Heterogenous OP-ELM Kernel Types	Linear, Gaussian, Sigmoid

The proposed LM-BP-based method achieved the highest average accuracy over all experiment runs compared to the other fourteen machine learning methods. The results are visualized in Figure 3 and summarized in Table 2.

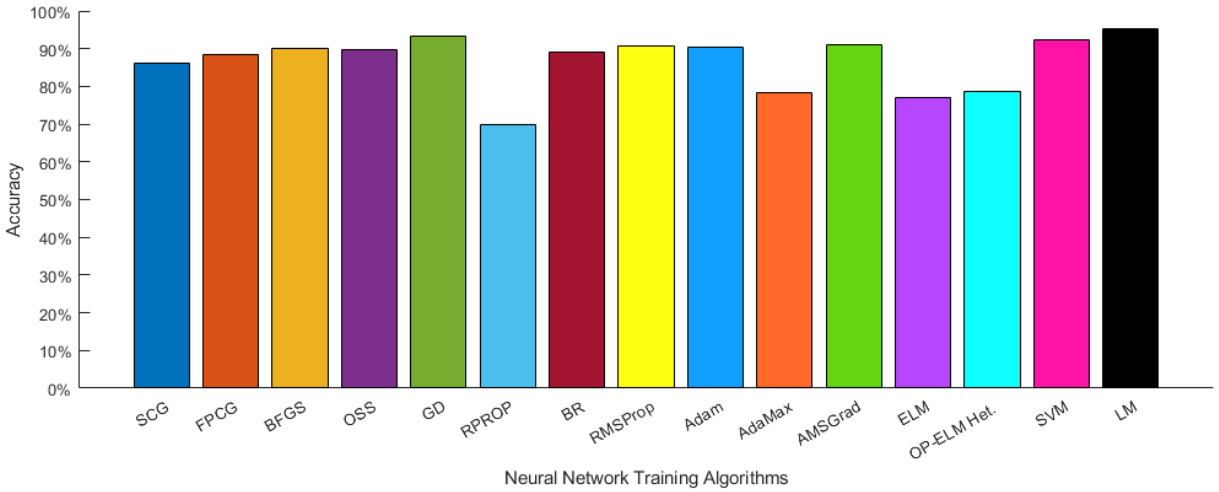

Figure 3. Experimental results plot. The proposed LM-BP-based system achieved the highest accuracy compared to fourteen existing machine learning algorithms.

Table 2. Comparison Results.

Parameter Name	Value
SCG-BP	86.21
FPCG-BP	88.55
BFGS-BP	89.61
OSS-BP	90.10
GD-BP	69.85
RPROP	93.28
RMSProp	90.59
Adam	90.54
AdaMax	78.47
AMSGrad	91.01
BR-BP	89.09
ELM	77.12
OP-ELM	78.74
SVM	92.36
LM-BP	95.12

Two statistical tests were conducted to investigate the proposed method's significance compared to the other fourteen methods. The first test involved creating an 80% confidence interval (CI) in each approach presented in Table 2, while the second test involved the creation of a 95% CI for each method. Then, the confidence intervals of the compared approaches were checked for overlaps with the CI from the LP-BP algorithm. If they do not overlap, it is a strong indication that the results from the LM-BP are statistically significant. The creation of the CI followed formula (8) where $\overline{x}$ is the samples average, Z is the standardized score ($Z = 1.282$ for an 80% CI while $Z = 1.96$ for a 95% CI), s is the sample's standard deviation and smp is the sample size.

$$\mathrm{CI} = \overline{x} \pm Z \frac{s}{\sqrt{smp}} \tag{8}$$

The results from the first statistical test can be seen in Figure 4, where it is shown that there is no overlap between the CI from the LM-BP algorithm and the other compared methods, which is interpreted as a strong indication that the results are statistically significant.

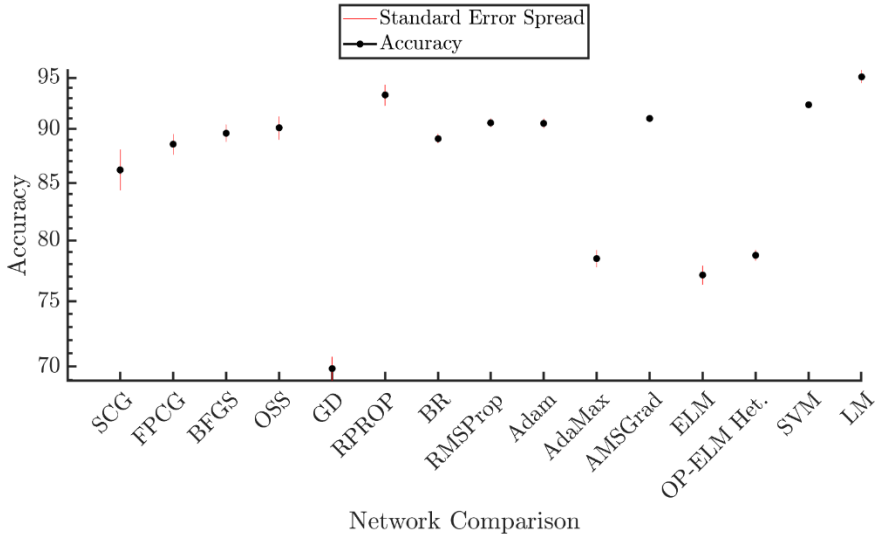

Figure 4. Statistical analysis of the results using an 80% CI. It can be seen from this figure that there is no overlap between the LM-BP algorithm and the other approaches, which is a strong indication that the results from the proposed method are statistically significant.

The results from the second statistical test can be seen in Figure 5. It is shown that there is no overlap between the CIs from the LM-BP algorithm and the other compared methods, which is interpreted as a strong indication that the results are statistically significant. One exception is the RPROP method which contains an overlap with the LM-BP algorithm. This overlap doesn't allow any conclusion on whether the results between these methods are statistically significant or not.

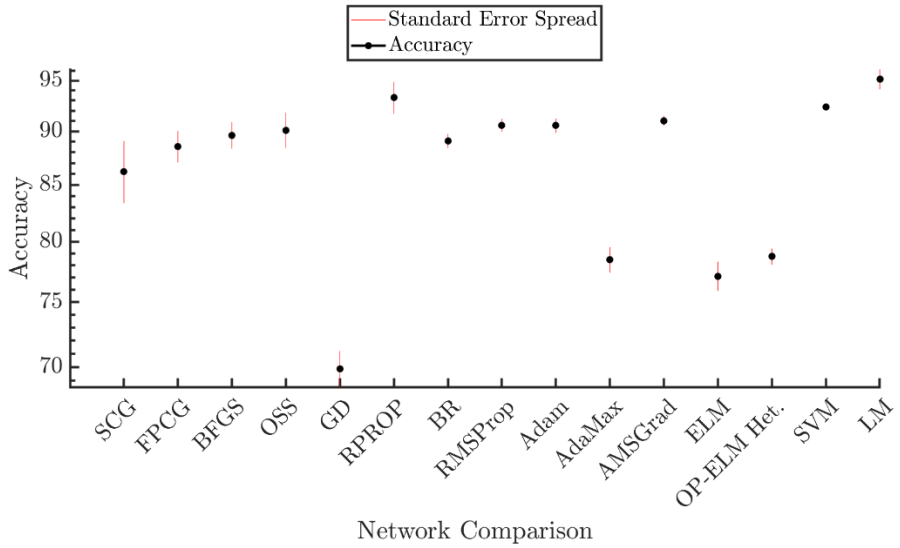

Figure 5. Statistical analysis of the results using a 95% CI. It can be seen from this figure that there is no overlap between the LM-BP algorithm and the other approaches, which is a strong indication that the results from the proposed method are statistically significant. One exception is the RPROP method, which overlaps with the LM-BP algorithm, which doesn't allow any conclusion regarding the statistical significance between the two methods.

6. Discussion

This article presents a system for automatically classifying the hemiplegia type between patients and healthy individuals. The system receives data from RehaGait's mobile gait analysis system accelerometer, which underwent a pre-processing and feature extraction procedure. Then, the extracted features create the input vector to an LM-BP-based classification algorithm, classifying them into three classes (healthy, left, or right hemiplegia). The experimental results from comparing the LM-BP-based method with fourteen different machine learning methods experimentally verified the proposed method's advantage over existing ones in terms of classification accuracy.

The proposed method was run one additional time. The results from this run were used to create the confusion matrix shown in Figure 6.

The LM-BP algorithm achieved a very high accuracy (95.8%). The number of test samples introduced to the network was 406 (132 for left hemiplegia, 219 for right hemiplegia, and 55 for non-patients). Each row defined the classification output of the network where the green boxes corresponded to correctly classified samples while the red boxes corresponded to incorrectly classified ones. The white box at the end of each row defined the percentage of all the samples predicted to belong to each class that was correctly (green color) and incorrectly (red color) classified. Each column defined the target class where the green boxes corresponded to correctly classified samples while the red boxes corresponded to incorrectly classified ones. At the end of each column, the white box defined the percentage of all the samples that belonged to each class and was correctly (green color) or incorrectly (red color) classified.

The true positive (TP), true negative (TN), false positive (FP), and false negative (FN) metrics can be calculated using the data from the confusion matrix. TP is the number of correctly classified positive class samples as positive. TN is the number of correctly

classified negative class samples as negative. FP is the number of incorrectly classified negative class samples as positive and FN is the number of incorrectly classified positive class samples.as negative. The TP, TN, FP, and FN are calculated for each class in a multi-class classification problem.

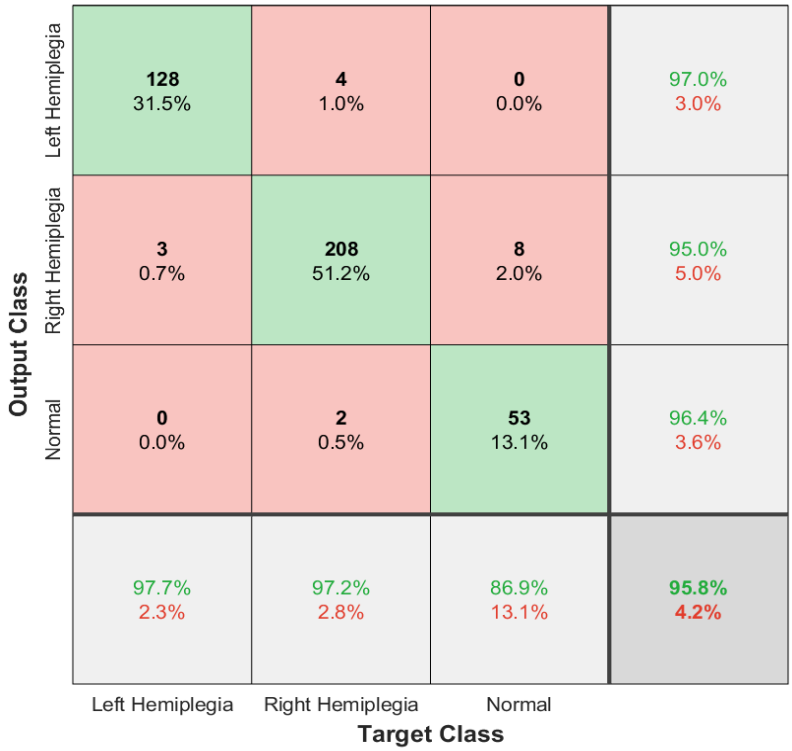

Figure 6. The confusion matrix. The green boxes show the correctly classified samples in this figure, while the red boxes show the misclassified ones. The vertical white boxes depict the percentages of all the samples predicted to belong to each class that is correctly (green color) and incorrectly (red color) classified. The horizontal white boxes depict the percentages of all the examples belonging to each class correctly (green color) and incorrectly (red color) classified. Finally, the grey box depicts the overall accuracy.

The above metrics were used to calculate the precision, recall, specificity, and F-score performance metrics. Precision shows what fraction of predictions as a positive class were actually positive and is calculated using the formula $\frac{TP}{TP+FP}$. Recall shows what fraction of all positive samples were correctly predicted as positive by the classifier and is defined using the equation $\frac{TP}{TP+FN}$. Specificity shows what fraction of all negative samples are correctly predicted as negative by the classifier and is calculated using the formula $\frac{TN}{TN+FP}$. Finally, F-score is a measure of a test's accuracy and combines the precision and recall metrics $\left(Fscore = 2\frac{precision \times recall}{precision+recall}\right)$. The precision, recall, specificity, and F-score performance metrics are summarized in Table 3. They show that the proposed method managed to get high scores in each class for all metrics.

Table 3. Performance Metrics.

	Precision	Recall	Specificity	F-Score
Left Hemiplegia	0.9771	0.9697	0.9891	0.9734
Right Hemiplegia	0.972	0.9498	0.9679	0.9607
Normal	0.8689	0.9636	0.9772	0.9138

The next figure depicts each class's receiver operating characteristic (ROC) curve. A ROC curve is a graphical plot describing the trade-off between true positive rate (sensitivity)

and false positive rate (1–specificity). If the curve is very close to the top left corner, it is an indication that the classifier has very good performance. On the other hand, if the curve is very close to the 45-degree diagonal of the ROC space, it indicates poor classification performance. All the curves in Figure 7 are very close to the upper left corner, and they have the area under the curve (AUC) values 0.9851 (left hemiplegia), 0.9772 (right hemiplegia), and 0.9919 (normal). Both observations show that the classifier has excellent classification performance (AUC values between 0.9 and 1 indicate an excellent performing classifier).

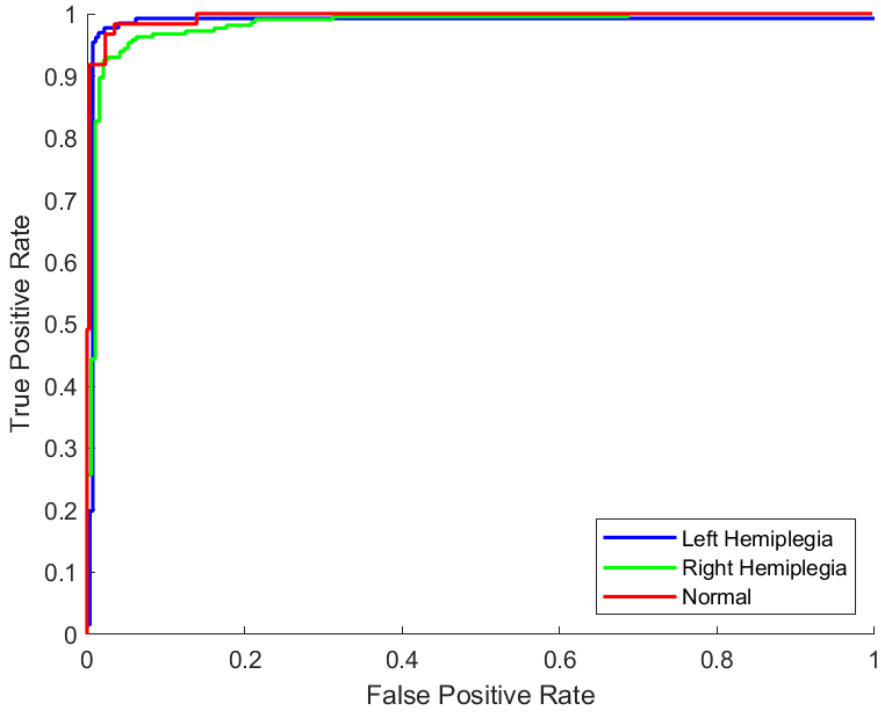

Figure 7. The ROC curves for each class. This figure depicts the ROC curves for left hemiplegic (blue color), right hemiplegic (green color), and normal subjects. All three curves are near the top left corner of the plot, which indicates a good-performing classifier.

The proposed system's main characteristic is its ability to distinguish between the two hemiplegic types (left or right) and achieve a high classification accuracy (95.12%). It utilizes the gait data from only ten healthy and twenty hemiplegic individuals. One limitation of the proposed method is the small number of participants, resulting in small dataset size. Another restriction of the proposed system is the limitation in one type of motor disability.

7. Conclusions

This study proposed an automated tool for classifying hemiplegic from non-hemiplegic patients and can also diagnose the hemiplegia type (right or left). The proposed automatic classification method achieved a high accuracy classification rate using the LM-BP algorithm. The obtained accuracy results were tested for their significance using 80% and 95% CIs. In the first test, they were found statistically significant compared to fourteen other popular machine learning methods. At the same time, it was statistically significant in thirteen out of fourteen cases in the second test. The CI of the LM-BP algorithm had an overlap with the CI of the RPROP algorithm, which didn't allow any conclusion on whether the results between these two algorithms are statistically significant.

Further plans for this project involve using a larger dataset containing more data from healthy and hemiplegic individuals. Including additional data would make the LM-BP classification algorithm more accurate and achieve an even higher classification accuracy. Future work involves expanding the dataset with more motor disability diseases like diplegia and Parkinson's disease. The addition of more diseases will allow the system

to recognize more motor disabilities, resulting in a complete system. This system can be used as a supplementary diagnostic tool by physiotherapists, allowing them to adapt their patient treatments automatically.

Author Contributions: Conceptualization, I.T., E.G. and N.G.; methodology, V.C., A.A. and I.T.; software, I.T. and A.A.; validation, A.T.T. and M.G.T.; investigation, C.G. and A.T.T.; data curation, D.V., D.D. and A.P.; writing—original draft preparation, V.C., A.A., D.D., D.V. and I.T.; writing—review and editing, I.T., A.T.T., C.G., M.G.T., E.G., A.P. and N.G.; visualization, V.C.; supervision, A.P. and N.G.; funding acquisition, A.P. and N.G. All authors have read and agreed to the published version of the manuscript.

Funding: We acknowledge support of this work by the project "MEGATRON" (MIS 5047227) which is implemented under the Action "Reinforcement of the Research and Innovation Infrastructure", funded by the Operational Programme "Competitiveness, Entrepreneurship and Innovation" (NSRF 2014-2020) and co-financed by Greece and the European Union (European Regional Development Fund).

Institutional Review Board Statement: The study was conducted according to the guidelines of the Declaration of Helsinki, and approved by Ethics Committee of University of Ioannina.

Informed Consent Statement: Informed consent was obtained from all subjects involved in the study. Written informed consent has been obtained from the patients to publish this paper.

Data Availability Statement: New data were created and analyzed in this study. Data sharing not applicable.

Conflicts of Interest: The authors declare no conflict of interest.

References

1. Davies, P.M. *Steps to Follow: The Comprehensive Treatment of Patients with Hemiplegia*; Springer Science & Business Media: Berlin/Heidelberg, Germany, 2000.
2. Ruskin, A.P. Understanding stroke and its rehabilitation. *Stroke* **1983**, *14*, 438–442. [CrossRef] [PubMed]
3. Donath, L.; Faude, O.; Lichtenstein, E.; Pagenstert, G.; Nüesch, C.; Mündermann, A. Mobile inertial sensor based gait analysis: Validity and reliability of spatiotemporal gait characteristics in healthy seniors. *Gait Posture* **2016**, *49*, 371–374. [CrossRef] [PubMed]
4. HASOMED. RehaGait—Mobile Gait Analysis. Available online: https://hasomed.de/en/products/rehagait/ (accessed on 3 September 2021).
5. Schwesig, R.; Fischer, D.; Lauenroth, A.; Becker, S.; Leuchte, S. Can falls be predicted with gait analytical and posturographic measurement systems? A prospective follow-up study in a nursing home population. *Clin. Rehabilit.* **2013**, *27*, 183–190. [CrossRef] [PubMed]
6. Lee, J.; Park, S.; Shin, H. Detection of Hemiplegic Walking Using a Wearable Inertia Sensing Device. *Sensors* **2018**, *18*, 1736. [CrossRef] [PubMed]
7. Ji, N.; Zhou, H.; Guo, K.; Samuel, O.W.; Huang, Z.; Xu, L.; Li, G. Appropriate mother wavelets for continuous gait event detection based on time-frequency analysis for hemiplegic and healthy individuals. *Sensors* **2019**, *19*, 3462. [CrossRef]
8. Pauk, J.; Minta-Bielecka, K. Gait patterns classification based on cluster and bicluster analysis. *Biocybern. Biomed. Eng.* **2016**, *36*, 391–396. [CrossRef]
9. Patil, S.; Shah, A.; Dalvi, S.; Sisodia, J. Early Detection of Hemiplegia by Analyzing the Gait Characteristics and Walking Patterns Using. In *Proceedings of the Soft Computing and Signal Processing, Proceedings of the 2nd ICSCSP 2019, Hyderabad, India, 21–22 June 2019*; Springer: Singapore, 2019; Volume 1118, p. 39.
10. Padilla, U. Fuzzy Classification of Hemiplegic Gait Using Kinematic Indicators in Knee. In Proceedings of the VI Latin American Congress on Biomedical Engineering CLAIB 2014 Paraná, Argentina, 29–31 October 2014; Springer: Cham, Switzerland, 2014; pp. 596–599.
11. Manca, M.; Ferraresi, G.; Cosma, M.; Cavazzuti, L.; Morelli, M.; Benedetti, M.G. Gait Patterns in Hemiplegic Patients with Equinus Foot Deformity. *BioMed Res. Int.* **2014**, *2014*, 1–7. [CrossRef]
12. Kim, J.; Oh, S.-I.; Cho, H.; Kim, H.S.; Chon, J.; Lee, W.J.; Shin, J.H.; Ahn, J.Y.; Kim, T.; Han, J.-S.; et al. Gait patterns of chronic ambulatory hemiplegic elderly compared with normal Age-Matched elderly. *Int. J. Precis. Eng. Manuf.* **2015**, *16*, 385–392. [CrossRef]
13. LeMoyne, R.; Kerr, W.; Mastroianni, T.; Hessel, A. Implementation of machine learning for classifying hemiplegic gait disparity through use of a force plate. In Proceedings of the 2014 13th International Conference on Machine Learning and Applications, Detroit, MI, USA, 3–6 December 2014; pp. 379–382.

14. Jung, S.; Bong, J.; Kim, S.-J.; Park, S. DNN-Based FES Control for Gait Rehabilitation of Hemiplegic Patients. *Appl. Sci.* **2021**, *11*, 3163. [CrossRef]
15. Yardimci, A. Fuzzy Logic Based Gait Classification for Hemiplegic Patients. In *International Symposium on Intelligent Data Analysis*; Springer: Berlin/Heidelberg, Germany, 2007; pp. 344–354.
16. Luo, H.; Luo, J. Evaluating the Intra-limb Coordination during Gait in Hemiplegia. In Proceedings of the 2018 IEEE International Conference on Cyborg and Bionic Systems (CBS), Shenzhen, China, 25–27 October 2018; pp. 612–615.
17. Wong, A.M.; Pei, Y.-C.; Hong, W.-H.; Chung, C.-Y.; Lau, Y.-C.; Chen, C.P. Foot contact pattern analysis in hemiplegic stroke patients: An implication for neurologic status determination. *Arch. Phys. Med. Rehabilit.* **2004**, *85*, 1625–1630. [CrossRef]
18. LeMoyne, R.; Mastroianni, T. Implementation of a smartphone as a wearable and wireless gyroscope platform for machine learning classification of hemiplegic gait through a multi-layer perceptron neural network. In Proceedings of the 2018 17th IEEE International Conference on Machine Learning and Applications (ICMLA), Orlando, FL, USA, 17–20 December 2018; pp. 946–950.
19. Aguilera, A.; Subero, A. Automatic gait classification patterns in spastic hemiplegia. *Adv. Data Anal. Classif.* **2020**, *14*, 897–925. [CrossRef]
20. Morbidoni, C.; Cucchiarelli, A.; Agostini, V.; Knaflitz, M.; Fioretti, S.; Di Nardo, F. Machine-learning-based prediction of gait events from EMG in cerebral palsy children. *IEEE Trans. Neural Syst. Rehabilit. Eng.* **2021**, *29*, 819–830. [CrossRef] [PubMed]
21. Agostini, V.; Knaflitz, M.; Nascimberi, A.; Gaffuri, A. Gait measurements in hemiplegic children: An automatic analysis of foot-floor contact sequences and electromyographic patterns. In Proceedings of the 2014 IEEE International Symposium on Medical Measurements and Applications (MeMeA), Lisboa, Portugal, 11–12 June 2014; pp. 1–4.
22. Di Nardo, F. EMG-based characterization of walking asymmetry in children with mild hemiplegic cerebral palsy. *Biosensors* **2019**, *9*, 82. [CrossRef]
23. McAloon, M.T.; Hutchins, S.; Twiste, M.; Jones, R.; Forchtner, S. Validation of the activPAL activity monitor in children with hemiplegic gait patterns resultant from cerebral palsy. *Prosthet. Orthot. Int.* **2014**, *38*, 393–399. [CrossRef] [PubMed]
24. Krzak, J.J.; Corcos, D.M.; Graf, A.; Smith, P.; Harris, G.F. Effect of fine wire electrode insertion on gait patterns in children with hemiplegic cerebral palsy. *Gait Posture* **2013**, *37*, 251–257. [CrossRef] [PubMed]
25. Wang, X.; Wang, Y. Gait analysis of children with spastic hemiplegic cerebral palsy. *Neural Regen. Res.* **2012**, *7*, 1578–1584.
26. Aguilera, A.; Subero, A.; Mata-Toledo, R. Application of Data Mining Techniques on EMG Registers of Hemiplegic Patients. In *Industrial Conference on Data Mining*; Springer: Berlin/Heidelberg, Germany, 2013; pp. 254–265.
27. Abaid, N.; Cappa, P.; Palermo, E.; Petrarca, M.; Porfiri, M. Gait detection in children with and without hemiplegia using single-axis wearable gyroscopes. *PLoS ONE* **2013**, *8*, e73152. [CrossRef]
28. Watanabe, T.; Miyazawa, T.A. Validation Test of a Simple Method of Stride Length Measurement Only with Inertial Sensors and a Preliminary Test in FES-assisted Hemiplegic Gait. In *World Congress on Medical Physics and Biomedical Engineering Toronto, Ontario, Canada*; Springer: Cham, Switzerland, 2015; pp. 1111–1114.
29. Granat, M.; Maxwell, D.; Bosch, C.; Ferguson, A.; Lees, K.; Barbenel, J. A body-worn gait analysis system for evaluating hemiplegic gait. *Med. Eng. Phys.* **1995**, *17*, 390–394. [CrossRef]
30. Ohnishi, T.; Iwasaki, T.; Tanaka, M. Evaluation of hemiplegia caused by stroke by using joint detection of depth sensors-case of SIAS. *Electr. Eng. Jpn.* **2019**, *206*, 33–43. [CrossRef]
31. Kumari, P.; Cooney, N.J.; Kim, T.-S.; Minhas, A.S. Gait analysis in Spastic Hemiplegia and Diplegia cerebral palsy using a wearable activity tracking device-a data quality analysis for deep convolutional neural networks. In Proceedings of the 2018 5th Asia-Pacific World Congress on Computer Science and Engineering (APWC on CSE), Nadi, Fiji, 10–12 December 2018; pp. 1–4.
32. Li, Q.; Wang, Y.; Sharf, A.; Cao, Y.; Tu, C.; Chen, B.; Yu, S. Classification of gait anomalies from kinect. *Vis. Comput.* **2018**, *34*, 229–241. [CrossRef]
33. Pandit, T.; Nahane, H.; Lade, D.; Rao, V. Abnormal gait detection by classifying inertial sensor data using transfer learning. In Proceedings of the 18th IEEE International Conference On Machine Learning And Applications (ICMLA), Boca Raton, FL, USA, 16–19 December 2019; pp. 1444–1447.
34. Azlan, W.N.W.; Zakaria, W.N.W.; Othman, N.; Mohd, M.N.H.; Ghani, M.N.A. Evaluation of Leap Motion Controller Usability in Development of Hand Gesture Recognition for Hemiplegia Patients. In Proceedings of the 11th National Technical Seminar on Unmanned System Technology 2019; Springer: Berlin/Heidelberg, Germany, 2021; pp. 671–682.
35. Cai, S.; Li, G.; Huang, S.; Zheng, H.; Xie, L. Automatic detection of compensatory movement patterns by a pressure distribution mattress using machine learning methods: A pilot study. *IEEE Access* **2019**, *7*, 80300–80309. [CrossRef]
36. Christou, V. Neural network-based approach for hemiplegia detection via accelerometer signals. In Proceedings of the 6th South-East Europe Design Automation, Computer Engineering, Computer Networks and Social Media Conference, Preveza, Greece, 24–26 September 2021.
37. Priya, S.J.; Rani, A.J.; Subathra, M.; Mohammed, M.A.; Damaševičius, R.; Ubendran, N. Local pattern transformation based feature extraction for recognition of Parkinson's disease based on gait signals. *Diagnostics* **2021**, *11*, 1395. [CrossRef] [PubMed]
38. Møller, M.F. A scaled conjugate gradient algorithm for fast supervised learning. *Neural Netw.* **1993**, *6*, 525–533. [CrossRef]
39. Levenberg, K. A method for the solution of certain non-linear problems in least squares. *Q. Appl. Math.* **1944**, *2*, 164–168. [CrossRef]
40. Marquardt, D.W. An Algorithm for Least-Squares Estimation of Nonlinear Parameters. *J. Soc. Ind. Appl. Math.* **1963**, *11*, 431–441. [CrossRef]

41. Scales, L. *Introduction to Non-Linear Optimization*; Macmillan International Higher Education: London, UK, 1985.
42. Hery, M.A.; Ibrahim, M.; June, L. BFGS method: A new search direction. *Sains Malays.* **2014**, *43*, 1591–1597.
43. Battiti, R. First-and second-order methods for learning: Between steepest descent and Newton's method. *Neural Comput.* **1992**, *4*, 141–166. [CrossRef]
44. Lemaréchal, C. Cauchy and the gradient method. *Doc. Math. Extra.* **2012**, *251*, 10.
45. Riedmiller, M.; Braun, H. A direct adaptive method for faster backpropagation learning: The RPROP algorithm. In Proceedings of the IEEE International Conference on Neural Networks, San Francisco, CA, USA, 28 March–1 April 1993; pp. 586–591.
46. MacKay, D.J. Bayesian interpolation. *Neural Comput.* **1992**, *4*, 415–447. [CrossRef]
47. Foresee, F.D.; Hagan, M.T. Gauss-Newton approximation to Bayesian learning. In Proceedings of the International Conference on Neural Networks (ICNN'97), Houston, TX, USA, 12 June 1997; Volume 3, pp. 1930–1935.
48. Tieleman, T.; Hinton, G. *Coursera: Neural Networks for Machine Learning-Lecture 6.5: RMSprop*; University of Toronto: Toronto, ON, Canada, 2012.
49. Kingma, D.P.; Adam, J.B. Adam: A method for stochastic optimizatio. In Proceedings of the International Conference on Learning Representations, San Diego, CA, USA, 7–9 May 2015.
50. Duchi, J.; Hazan, E.; Singer, Y. Adaptive subgradient methods for online learning and stochastic optimization. *J. Mach. Learn. Res.* **2011**, *12*, 7.
51. Huang, G.-B.; Zhu, Q.-Y.; Siew, C.-K. Extreme learning machine: Theory and applications. *Neurocomputing* **2006**, *70*, 489–501. [CrossRef]
52. Miche, Y.; Sorjamaa, A.; Bas, P.; Simula, O.; Jutten, C.; Lendasse, A. OP-ELM: Optimally pruned extreme learning machine. *IEEE Trans. Neural Netw.* **2009**, *21*, 158–162. [CrossRef] [PubMed]
53. Zahir, N.; Mahdi, H. Snow depth estimation using time series passive microwave imagery via genetically support vector regression (case study urmia lake basin). *ISPRS—Int. Arch. Photogramm. Remote Sens. Spat. Inf. Sci.* **2015**, *40*, 555–558. [CrossRef]
54. Farias, F.S., Jr.; Azevedo, R.A.; Rivera, E.C.; Herrera, W.E.; Rubens, F.M.; Lima, L.P., Jr. Product Quality Monitoring Using Extreme Learning Machines and Bat Algorithms: A Case Study in Second-Generation Ethanol Production. In *Computer Aided Chemical Engineering*; Elsevier: Amsterdam, The Netherlands, 2014; Volume 33, pp. 955–960.